Studies of Lidar Calibration for the Next Generation of Imaging Atmospheric Cherenkov Telescopes

Sam Nolan*and Cameron Rulten* for the CTA Consortium

**Physics Department, Durham University, South Road, Durham, County Durham, DH1 3LE*

***Abstract*. The next generation of ground-based imaging atmospheric Cherenkov telescope arrays (AGIS, CTA) seek an energy threshold of some 10's of GeV whilst minimising systematic uncertainty in derived flux and energy. To achieve this a detailed study of atmospheric quality is required. In this work we shall present a simulation study using an array comprising 97 telescopes, folded with real lidar data, to show the effect of changing atmospheric quality on a reconstructed gamma-ray spectrum. This work forms part of the design study performed by the atmospheric and calibration working group of the CTA consortium.**

***Keywords*: gamma-ray, CTA, atmosphere**

I. Introduction

The current generation of imaging atmospheric Cherenkov telescopes have revealed a signficant number of sources emitting in the energy range from 60 GeV to 40 TeV [1]. The next generation of telescope array systems (CTA, AGIS) aim to increase the flux sensitivity by 1 order of magnitude, whilst increasing the energy coverage from some tens of GeV to a few hundred TeV [2] [3]. Whilst increasing the number of astrophysical objects from known gamma-ray source classes, this next step should also observe many new classes of object previously unobserved in the gamma-ray waveband. As the technique is calorimetric in nature, the clarity of the atmosphere must be accounted for when deriving fluxes and extracting spectra. A significant aerosol population in the atmosphere will lower the Cherenkov photon yield from a shower of given impact parameter and energy, thus dimming the images seen by the telescope cameras, and (if uncorrected for) the gamma-ray event will be attributed a lower energy than it actually has [4]. This systematic effect can be removed by, to first order, using the cosmic-ray background trigger rate of the telescope systems as an atmospheric clarity measure [5]. Although muon data may also be used in calibration, it samples only the atmospheric clarity in the immediate vicinity of the telescope system. On the other hand, optical telescopes which perform starlight monitoring sample the integrated clarity of the entire atmosphere, again making them non-ideal as the only source of calibration information for an imaging Cherenkov telescope. In this short paper, an alternative approach is suggested. A single scattering lidar operating around the position of the maximum in the spectrum of Cherenkov light seen by the telescopes (355nm) has the ability to calculate the longitudinal transmission (T) of the atmosphere, this may then be folded into the simulations of the telescope system, from which lookup tables for parameters such as reconstructed energy, effective area and mean-scaled length and width are derived. Using such a lidar deployed on the Namibian highlands, and folding its derived transmission profiles with simulations of a 97 telescope design, the effect of changing atmospheric quality on the reconstructed spectrum of simulated gamma-rays is studied.

II. Lidar

Measurements of the atmosphere were recorded using the Easy-Lidar ALS450XT developed with and manufactured by Leosphere France. The Easy-Lidar ALS450XT is a monostatic bi-axial lidar which operates at a wavelength of 355nm. The lidar emits laser pulses at a frequency of up to 20Hz and detects the backscattered signal using a photomultiplier tube (PMT). The lidar can detect to a range of nearly 20 kilometres with a spatial resolution of approximately 1.5 metres [6]. The lidar has been pointed toward zenith and a single atmospheric profile is averaged over 600 laser shots. For this research 10 profile runs were generated at twilight on 2 nights, July 25th 2008, when sky clarity was visibly clear, and August 15th 2008 when sky clarity was perceived to be visibly poor (hitherto refered to as clear and hazy). Transmission data were then extracted from the lidar using a Klett inversion method [7]. It should be noted however, that the longitudinal transmission profile produced is at a single wavelength only, and detailed modelling is performed using MODTRAN (version 4) to match this profile to a model. MODTRAN (MODerate resolution atmospheric TRANsmission) is a computer program designed to model atmospheric propagation of electromagnetic radiation from approximately 100 nm to - 1 mm with a spectral resolution of 1% [8]. The MODTRAN simulation code has been used to produce all models of vertical aerosol structure (plus the molecular absorption and scattering) cited within this paper. The aerosol desert dust model within MODTRAN introduces a uniform layer of aerosols (mostly sand particles) of height 2 km directly above the ground level, whose density is then increased as the wind speed parameter is increased. By tuning this parameter to the lidar responses from the clear and hazy nights separately, a model for the transmission profile on each night was derived.

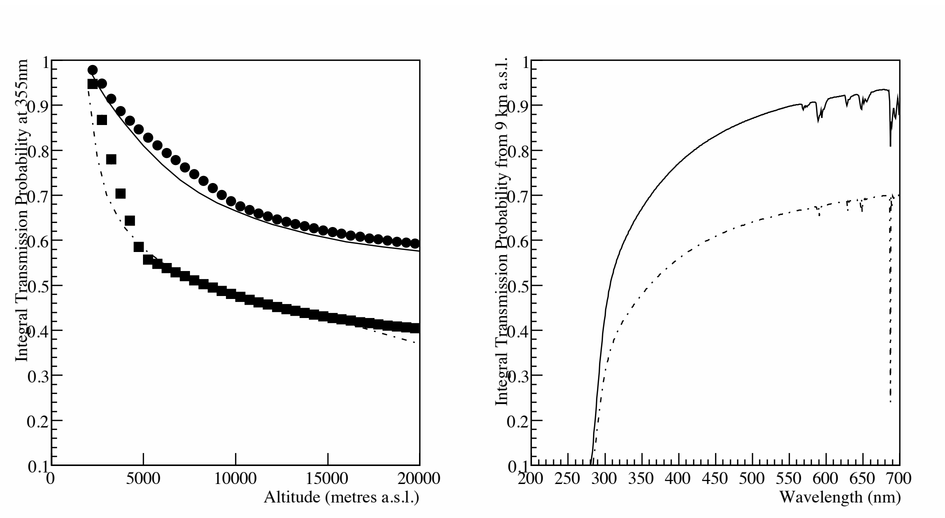

Fig. 1. *Left*: The lidar derived atmospheric profile (circular points) and MODTRAN fit (solid line) for July 25th (clear) and lidar derived atmospheric profile (square points) and MODTRAN fit (dashed line) for August 15th (hazy) are shown in terms of integrated transmission probability at 355nm versus altitude. *Right:* The MODTRAN fits for July 25th (solid line) and August 15th (dashed line) shown in the left panel, are plotted as integrated transmission probability at 9 km above sea-level (around the maximum in Cherenkov emission) versus photon wavelength.

III. Telescope Simulations

A series of 20 million gamma-ray showers between 5 GeV and 2 TeV, with a differential spectrum of form $E^{-2.0}$ at zenith were produced with CORSIKA, and the response of a 97 telescope array was produced using the sim_telarray package [9]. At the telescope simulation stage the derived atmospheric transmission models were folded in, so two different databases of telescope responses were produced, one for the clear night, and one for the hazy night. The 97 telescope system consisted of 12 large parabolic dish telescopes with a mirror area of 600 m^2 and with 4093 pixels at their primary focus of 35 metres, giving a 5^o field of view. In addition 85 medium Davies-Cotton dish telescopes each with a mirror area of 100 m^2 and with 1735 pixels at their primary focus of 15 metres, giving a 7^o field of view, were also simulated. The layout of these telescopes can be seen in Figure 2.

In addition the quantum efficiency of the PMT's in both telescopes was increased by 50% as compared to the Photonis XP2960, and a trigger threshold of 3 pixels each having a 5.3 photoelectron signal (all within a given sector of the camera) was set, events failing to meet this criteria were discarded. Figure 3 shows the effective area for the simulated telescope system derived from both databases of telescope simulations (clear atmosphere and hazy atmosphere) for both events which trigger, and events which pass loose quality cuts of at least 2 triggering telescopes, with a minimum of 4 signal tubes in each camera. In addition, the right panel of Figure 3 shows the effective areas folded with a power-law spectrum of $E^{-2.45}$, to indicate the threshold energy of the system. For the hazy dataset, the triggering threshold energy is 10 GeV, rising to 20 GeV post the loose cuts. Whereas for the hazy dataset the minimum triggering

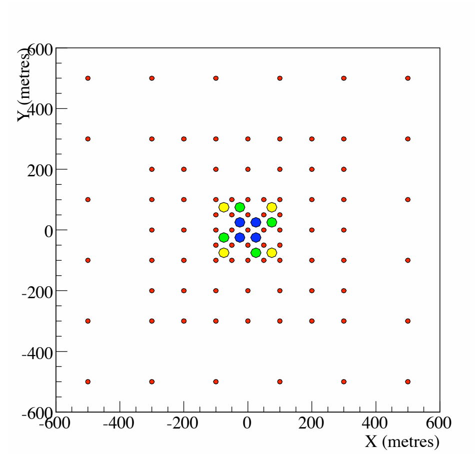

Fig. 2. Scaled image of simulated telescope layout, distances are on the ground. The larger (600 m^2) dishes are represented by the larger circles clustered towards the centre of the image, in order to capture a significant fraction of the Cherenkov photons from lower energy showers, and thus lower the energy threshold of the system.

threshold is 20 GeV rising to 30 GeV post the loose cut. At first sight a changing atmosphere appears to have little effect on the simulation, but this is misleading and doesn't illustrate the complete picture [10]. To perform a reconstruction of the energy of an event, in order to perform spectroscopy, one typically uses a lookup table based on simulation to derive the energy as a function of the impact parameter (r) and the the logarithm of the image brightness (S), this can be represented as a function E(r, S) [11] . However, S is a function of both energy and atmospheric transmission (T), represented as S(E, T). Thus the observed Cherenkov image brightness (size) is also dependent on atmospheric quality as well as energy. For the hazy dataset the size of an event, for

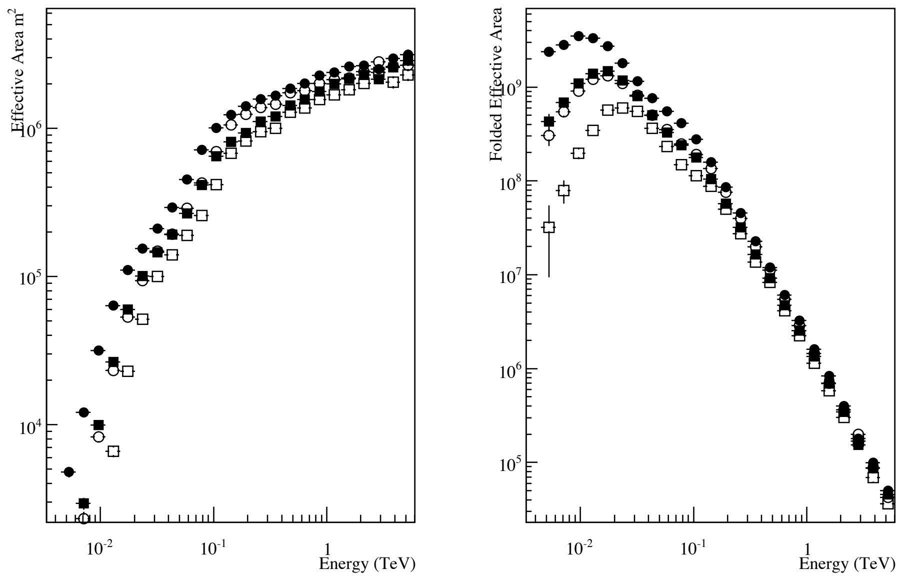

Fig. 3. *Left:* The effective area is shown for a database of gamma−ray showers at zenith folded with a telescope simulation with different models of the atmospheric quality based on lidar data by the clear(filled circles) and hazy (filled squares). In addition a cut of at least 2 triggering telescopes, with a minimum of 4 signal tubes is applied to the data, and the effective area after this cut for both atmospheric classes is shown by the clear (open circles) and hazy (open squares). *Right:* The plots from the left panel are folded with a power-law spectrum of $E^{-2.45}$, the energy thresholds of the system are then indicated by the peak of each plot.

a shower of given impact distance and energy, will be less compared to that using the clear dataset.

IV. RESULTS

In order to test the affect of atmospheric clarity on the simulated dataset, a set of lookup tables for the reconstructed energy $E_R(r, S)$ and the reconstructed effective area $A_R(E)$ were drawn from the simulation database for both clear and hazy atmospheres. A test spectrum of 100,000 events with a simulated energy E, and spectral shape $E^{-2.3}$, was then drawn randomly from each database. For these events $E_R(r, S)$ and $A_R(E)$ were derived from the lookup tables and a reconstructed differential spectrum was formed for the three specific combinations of simulations and lookup tables given in Table I.

TABLE I
THE SOURCES OF LOOKUP TABLES AND SIMULATED INPUT SPECTRA USED TO STUDY THE AFFECT OF ATMOSPHERIC CLARITY ON RECONSTRUCTED SPECTRA SHOWN IN FIGURE 4.

Case	Simulated Derived From	Lookup Derived From
1	Clear Database	Clear Database
2	Hazy Database	Clear Database
3	Hazy Database	Hazy Database

The reconstructed spectra are shown in Figure 4 and the lidar data together with the MODTRAN fits used to extract the transmission models applied in each case are shown in Figure 1.

V. DISCUSSION

As can be seen in Table II without correction the effects of varying atmospheric quality on the simulated telescope response is quite striking, leading to a significant shift in the reconstructed spectrum. This is largely due a shift in the size of all images, leading to the energy of any given event being reconstructed to an incorrect value. This is indicated in Table II where a power law fit of form $\frac{dN}{dE} = I_o E^{-\alpha}$ is fit to the data. Where dN/dE is the differential photon flux in events $m^{-2}TeV^{-1}$ is fit to the data in Figure 4.

TABLE II
SHOWING THE VALUES RETURNED FROM POWER-LAW FITTING TO THE RECONSTRUCTED SPECTRA FOR THE CASES LISTED IN TABLE I.

Case	I_o 1×10^{-11} m^{-2} TeV^{-1}	α
1	197±3	1.93±0.01
2	59±2	2.34±0.01
3	210±3	1.91±0.01

After correction (Table II, case 3), it can be seen that the power law fit is quite similar to that derived from a clear night (Table II, case 1), thus indicating that a lidar can be a useful tool in correcting data in ground-based gamma-ray astronomy. However, the transmission calculated from a single scattering lidar using Klett inversion is reported to have an associated systematic uncertainty up to around 30% [12]. Therefore the CTA design study atmospheric and calibration

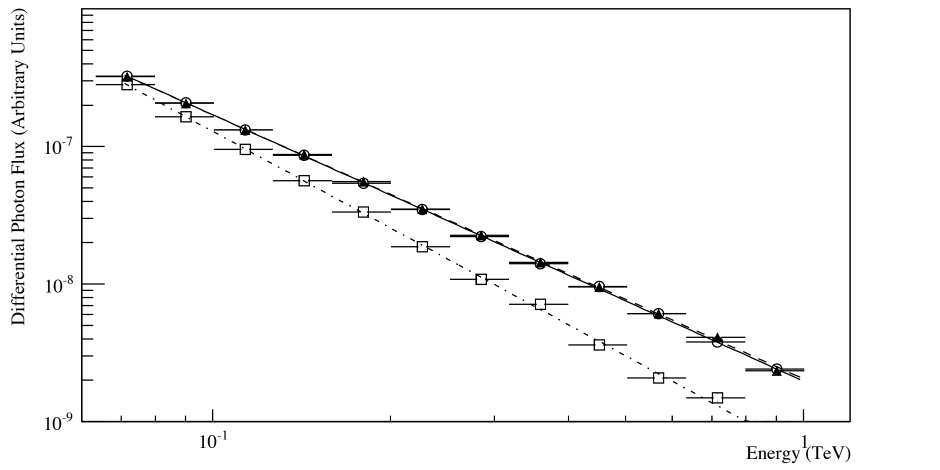

Fig. 4. Using lookups (for energy and reconstructed effective area) generated from a full simulation database a randomly sampled spectrum of 100,000 events with spectral slope of $E^{-2.3}$ is drawn from the database. These events are then reconstructed using the lookup tables, and a reconstructed spectrum is derived. This is repeated using the combinations of spectral source and lookup source given in Table I. The open circles show the reconstructed differential spectrum for case 1, the open squares for case 2 and the closed triangles for case 3. As case 3 shows, incoporating lidar data into the reconstruction allows a corrected spectrum to be formed with the approximately the same normalisation and slope as for a clear night, as exemplified by case 1.

working group are seeking to test whether a Raman lidar (with around 5% systematic uncertainty) would be better for atmospheric calibration. In addition, a detailed monte-carlo simulation study is underway to optimise the design of the CTA arrays. Studies into the affect of atmospheric quality will be ongoing, incorporating not just gamma-ray simulations, but also charged cosmic-ray simulations.

VI. Conclusion

Ground-based imaging atmospheric Cherenkov astronomy is calorimetric and must account for atmospheric quality when performing spectroscopy. Currently this is performed by appealing to the rate of background cosmic-rays, and data with sub-standard atmospheric quality is largely discarded. However, by utilising a ground-based lidar to probe the longitudinal atmospheric transmission to around the maximum of Cherenkov light production and beyond, the simulation results herein indicate that varying atmospheric quality may be corrected for, which may significantly increase the active lifetime of next generation ground-based gamma-ray observatories, such as CTA & AGIS, in addition to lowering systematic uncertainties in derived flux. Further work is currently underway to test this hypothesis using the current generation of instruments, such as H.E.S.S and MAGIC [11], [13].

Acknowledgements The support of the U.K. Science and Technology Facilities Council (STFC) and the technical staff at the University of Durham is gratefully acknowledged.

References

[1] Chadwick, P. et al., (2008), J. Phys. G, **35**, 033201
[2] Hermann, G. et al., (2008), , Proceedings of 30th ICRC, **03**, 1313
[3] Buckley, J. et al., (2008), e-Print: arXiv:0810.0444 [astro-ph]
[4] Nolan, S. et al., (2008), Proceedings of 30th ICRC, **03**, 1009
[5] Holder, J. & Le. Bohec, S., (2003), Astroparticle Physics, **19**, 221
[6] http://www.leosphere.com
[7] Klett, J., (1985), Applied Optics, **24**, 1638
[8] Kneizys F.X., et al., (1996), The MODTRAN 2/3 Report and LOWTRAN 7 Model, (Phillips Laboratory, Hanscom AFB, MA 01731, USA)
[9] Bernlöhr K., (2008), arXiv:0810.5722
[10] Daniel, M.K., (2008), Proceedings of 30th ICRC, **03**, 1329
[11] Aharonian, F. et al., (2006), A. & A., **457**, 899
[12] Papayannis, A & Fokitis, E., PAO Internal Note, 1998, Gap-Index No. 1998-018
[13] Ferenc, D et al., (2005), NIM A, **553**, 274